Journal of Theoretical and Applied Information Technology
31st August 2014. Vol. 66 No.3

ISSN: 1992-8645 www.jatit.org E-ISSN: 1817-3195

MODELLING AND SIMULATION OF SWITCHING FREQUENCY CONTROLLED REGULATED DISCONTINUOUS CONDUCTION MODE BOOST RECTIFIERS

[1]B.K.SHOBANA, [2]DR.P.RENUGA
[1]Part time Research Scholar, Department of EEE, Thigarajar College of Engineering, Madurai, India
[2]Associate Professor, Department of EEE, Thigarajar College of Engineering, Madurai, India
E-mail: [1]shobanabk@gmail.com, [2]preee@tce.edu

ABSTRACT

Regulated one switch boost rectifiers operating at a boundary of continuous and discontinuous modes is modelled. Proposed PWM and variable frequency control technique is used to reduce harmonics in the source current and also to regulate the output voltage. Small signal modeling is done for the design of boost rectifier and also for its control technique. The proposed control technique had the main advantage of reduced THD. The simulation is performed using MATLAB/SIMULINK software for the control methods.

Keywords: - *Boost rectifiers, Switching frequency, DCM, Duty cycle, Small signal Analysis*

1. INTRODUCTION

Boost converter also known as step up power converter which takes lower input voltage and produces higher output voltage. For AC/DC applications boost rectifier (rectifier feeding the boost converter) is used as pre-regulators. Generally boost converters are operated in continuous conduction mode to get higher input power factor and low Total Harmonic Distortion (THD) [1], [2] at the cost of complex and costlier circuit. Compared to this only one control loop is needed to regulate the output voltage in the Discontinuous Conduction Mode (DCM) with the absence of reverse recovery problem in the diode [3]-[6] .The two control methods in DCM are fixed switching frequency and variable switching frequency method and the comparison reveals the advantages of the proposed control scheme such as low Total Harmonic Distortion (THD) and better output voltage regulation.[7].With the use of small input capacitor in both the control methods high order harmonics due to discontinuous input current can be filtered and also to reduce low order harmonics a control method is given in [8].Within a fixed switching period duty cycle is varied such that rectifier is operated at the boundary of DCM and Continuous Conduction Mode (CCM) but the disadvantage is that the output voltage cannot be regulated. But in this paper output voltage regulation together with harmonic reduction is obtained.

2. BOOST CONVERTER BASICS

Boost Converter as shown in Fig.1 consists of four main elements namely controllable semiconductor switch S, diode D, inductor L and an output capacitor C_o. The input capacitor C_i is used to suppress the higher order harmonics of i_L.Fig.1 (b) represents the n^{th} pulse of i_L and inductor voltage V_L in that switching period.$\Delta_1 T_s$ is the time required for the inductor current to reach zero from its maximum value. The main concept in the boost converter is that when switch is closed there is increase in inductor current and the load gets separated from the input supply. When switch is opened still there is current flow, diode D is forward biased and so the current flows into the capacitor and the load that is output stage receives energy from the inductor and also from the input.

Journal of Theoretical and Applied Information Technology
31st August 2014. Vol. 66 No.3

ISSN: 1992-8645 www.jatit.org E-ISSN: 1817-3195

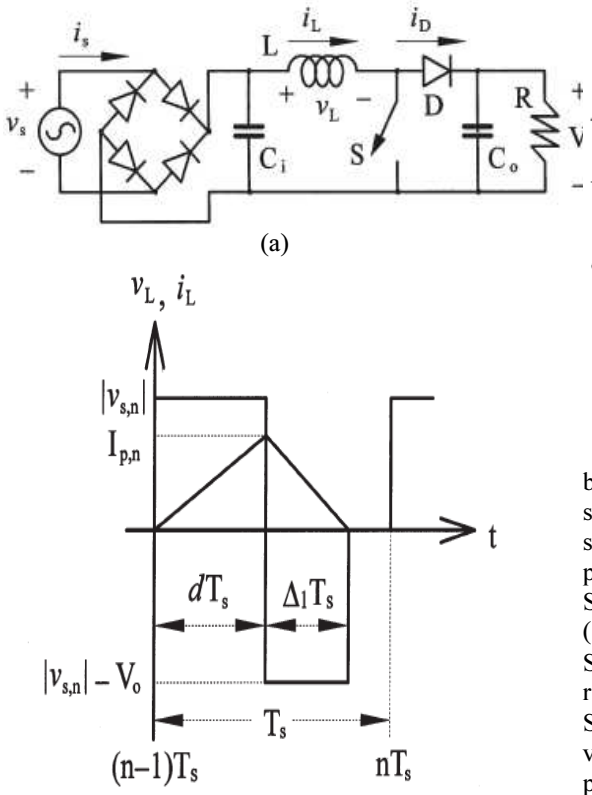

Figure 1: (a) Boost Rectifier and (b) i_L and v_L in the n^{th} switching period

3. SMALL SIGNAL ANALYSIS

Small signal modeling is performed to facilitate the design process of a proposed rectifier system. The goal of this analysis is to obtain a small signal transfer function $\hat{V}_o(s)/\hat{V}_{con}(s)$, where $\hat{V}_o$ and $\hat{V}_{com}$ are the small perturbations in the output voltage and control voltage respectively. Here the rectifier system operating in the discontinuous mode is discussed. Fig. 2 and Fig. 3 are the equivalent circuits during turn on and turn off intervals which are very much essential for the small signal analysis.

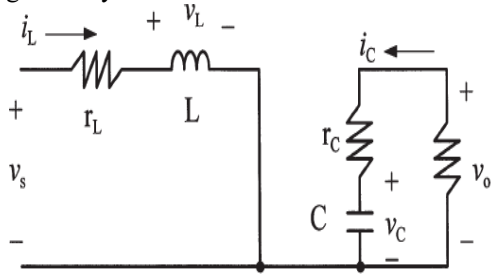

Figure 2: Equivalent circuit during turn on

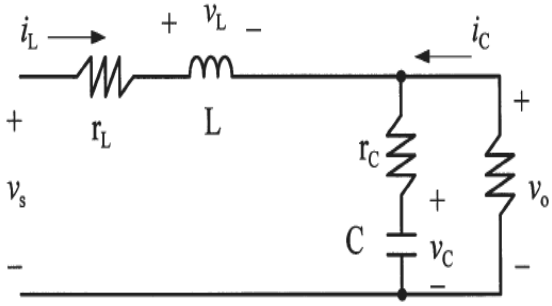

Figure 3: Equivalent circuit during turn off

The rectified input voltage can be replaced by its RMS value in small signal modeling. The small signal analysis can be deduced with the state space averaging technique to facilitate the design process [9], [10], [11].The Procedure is as follows:

Step1: State equations for each circuit state (interval).

Step2: Average the State equations using the duty ratio 'D' over a switching cycle.

Step3: Introduce small perturbations in state variables and separate AC and DC equations and proceed with AC equations alone. .

Step4: Transform AC equations into s-domain to solve for the transfer function.

Large signal analysis results are given below:

$$\begin{bmatrix} i_L' \\ v_c' \end{bmatrix} = \left[A^{ON}d + A^{OFF}(1-d) \right] \begin{bmatrix} i_L \\ v_c \end{bmatrix} + \left[B^{ON}d + B^{OFF}(1-d) \right] v_s \quad (1)$$

$$v_o = \left[C^{ON}d + C^{OFF}(1-d) \right] \begin{bmatrix} i_L \\ v_c \end{bmatrix} \quad (2)$$

Where the expressions of the six coefficient matrices are

$$A^{ON} = \begin{bmatrix} \frac{-r_L}{L} & 0 \\ 0 & -\frac{1}{C(R+r_c)} \end{bmatrix} \quad ; B^{ON} = \begin{bmatrix} \frac{1}{L} \\ 0 \end{bmatrix}$$

$$C^{ON} = \begin{bmatrix} 0 & \frac{R}{(R+r_c)} \end{bmatrix} \quad ; D^{ON} = \begin{bmatrix} 0 \end{bmatrix}$$

$$A^{OFF} = \begin{bmatrix} \frac{-R(r_c+r_L)+r_L r_c}{L(R+r_c)} & \frac{-R}{L(R+r_c)} \\ \frac{R}{C(R+r_c)} & \frac{-1}{C(R+r_c)} \end{bmatrix}$$

Journal of Theoretical and Applied Information Technology
31st August 2014. Vol. 66 No.3

ISSN: 1992-8645 www.jatit.org E-ISSN: 1817-3195

$$B^{OFF} = \begin{bmatrix} \frac{1}{L} \\ v_c \end{bmatrix}; \quad C^{OFF} = \begin{bmatrix} \frac{R}{(R+r_c)} r_c & \frac{R}{(R+r_c)} \end{bmatrix}$$

In (1) and (2), d is the instantaneous duty cycle, which is defined as

$$d = D + \hat{d} = \frac{t_{ON}}{t_s} = \frac{T_{ON} + \hat{t}_{ON}}{T_s + \hat{t}_s} \quad (3)$$

After the second order terms are neglected $\hat{d}$ can be expressed as

$$\hat{d} = \frac{1}{T_s}\hat{t}_{on} - \frac{T_{ON}}{T_s^2}\hat{t}_s \quad (4)$$

In (3) and (4), lower case letters are instantaneous values, the steady state quantities are represented by the uppercase letters, and lowercase letters with caps mean small perturbations. In the boundary of DCM control, the peak value of the inductor current equals to twice the average value then

$$2i_L = \frac{(t_s - t_{ON})(v_o - v_s)}{L} \quad (5)$$

From the above equation after the second order effects are neglected, $\hat{t}_{ON}$ can then be expressed as

$$\hat{t}_{ON} = -\frac{2L}{(V_o - V_s)}\hat{i}_L - \frac{2LI_L}{(V_o - V_s)^2}\hat{v}_s + \hat{t}_s + \frac{2LI_L}{(V - V_s)^2}\hat{v}_o \quad (6)$$

By introducing small perturbations into (1) and (2) and then substituting $\hat{d}$ with (4) and $\hat{t}_{ON}$ with (6), we can obtain

$$\begin{bmatrix} \hat{i}_L \\ \hat{v}_C \\ \hat{v}_o \end{bmatrix} = K \begin{bmatrix} \hat{i}_L & \hat{v}_C & \hat{v}_s & \hat{t}_s & \hat{v}_o \end{bmatrix}^T \quad (7)$$

Where K is a 3×5 co-efficient matrix. The expressions for k_{ij} are given in the Table 1. Of which the matrix elements k_{ij} are functions of the circuit parameters and steady state quantities of the circuit variables. Appling Laplace transformation to both sides of equations (1) and (2) and after rearranging the equations as we obtain equation (8)

Table1 :Expressions for k_{ij}

K11	$A_{11}^{on}D + A_{11}^{off}(1-D) - \frac{2L}{(V_o - V_s)T_s}[(A_{11}^{on} - A_{11}^{off})I_L + (A_{12}^{on} - A_{12}^{off})V_c$
K12	$A_{12}^{on}D + A_{12}^{off}(1-D)$
K13	$B_{11}^{on}D + B_{11}^{off}(1-D) - \frac{2LI_L}{(V_o - V_s)^2 T_s}[(A_{11}^{on} - A_{11}^{off})I_L + (A_{12}^{on} - A_{12}^{off})V_c]$
K14	$\frac{1}{T_S}(A_{11}^{on}I_L + A_{12}^{on}V_C + B_{11}^{off}V_S)$
K15	$\frac{2LI_L}{(V_o - V_s)^2 T_s}[(A_{11}^{on} - A_{11}^{off})I_L + (A_{12}^{on} - A_{12}^{off})V_C]$
K21	$A_{21}^{on}D + A_{21}^{off}(1-D) + \frac{2LI_L}{(V_o - V_s)T_s}A_{21}^{off}$
K22	$A_{22}^{on}D + A_{22}^{off}(1-D)$
K23	$B_{21}^{on}D + B_{21}^{off}(1-D) - \frac{2LI_L}{(V_o - V_s)^2 T_s}[(A_{21}^{on} - A_{21}^{off})I_L + (A_{22}^{on} - A_{22}^{off})V_c]$
K24	$\frac{1}{T_S}(A_{21}^{on}I_L + A_{22}^{on}V_C + B_{21}^{off}V_S)$
K25	$\frac{2LI_L}{(V_o - V_s)^2 T_s}[(A_{21}^{on} - A_{21}^{off})I_L + (A_{22}^{on} - A_{22}^{off})V_C + (B_{21}^{on} - B_{21}^{off})V_S]$
K31	$C_{11}^{on}D + C_{11}^{off}(1-D) - \frac{2L}{(V_o - V_s)T_s}[(C_{11}^{on} - C_{11}^{off})I_L + (C_{12}^{on} - C_{12}^{off})V_c]$
K32	$C_{12}^{on}D + C_{12}^{off}(1-D)$
K33	$-\frac{2LI_L}{(V_o - V_s)^2 T_s}[(C_{11}^{on} - C_{11}^{off})I_L + (C_{12}^{on} - C_{12}^{off})V_C]$
K34	$\frac{1}{T_S}(C_{12}^{off}V_C - V_O)$
K35	$\frac{2LI_L}{(V_o - V_s)^2 T_s}[(C_{11}^{on} - C_{11}^{off})I_L + (C_{12}^{on} - C_{12}^{off})V_C]$

$$\hat{I}_L(s) = \frac{k_{12}\hat{V}_c(s) + k_{13}\hat{V}_s(s) + k_{14}\hat{T}_s(s) + k_{15}\hat{V}_o(s)}{s - k_{11}} \quad (8)$$

$$\hat{V}_c(s) = \frac{k_{21}\hat{I}_L(s) + k_{23}\hat{V}_s(s) + k_{24}\hat{T}_s(s) + k_{25}\hat{V}_o(s)}{s - k_{22}} \quad (9)$$

$$\hat{V}_s(s) = \frac{k_{31}\hat{I}_L(s) + k_{32}\hat{V}_c(s) + k_{33}\hat{V}_s(s) + k_{34}\hat{T}_s(s)}{1 - k_{35}} \quad (10)$$

ISSN: 1992-8645 www.jatit.org E-ISSN: 1817-3195

Substituting (8) and (9) into (10) and letting $\hat{V}_s(s) = 0$,a small signal transfer function relating the output voltage and the switching period are as follows

$$\frac{\hat{V}_0(s)}{\hat{T}_s(s)} = \frac{b_2 s^2 + b_1 s + b_0}{a_2 s^2 + a_1 s + a_0} \quad (11)$$

where a_i and b_i are the functions of k_{ij} and listed in Table 2

Table 2: a_i and b_i in terms of k_{ij}

a_0	$(1-K_{35})(K_{11}K_{22}-K_{12}K_{21})+K_{31}(K_{15}K_{22}-K_{12}K_{25})+K_{32}(K_{25}K_{11}-K_{21}K_{15})$
a_1	$-(1-K_{35})(K_{11}+K_{22})-K_{31}K_{15}+K_{32}K_{25}$
a_2	$(1-K_{35})$
b_0	$K_{34}(K_{11}K_{22}-K_{12}K_{21})+K_{31}(K_{12}K_{24}-K_{14}K_{22})+K_{32}(K_{21}K_{14}-K_{24}K_{11})$
b_1	$-K_{34}(K_{11}+K_{22})+K_{31}K_{14}+K_{32}K_{24}$
b_2	K_{34}

For a PWM controller, assuming that the amplitude of the triangular carrier is A_T in volts and the switching frequency f_s in hertz, then the small signal transfer function from the switching period to the control voltage $\hat{V}_{con}(s)$ is

$$\frac{\hat{T}_s(s)}{\hat{V}_{con}(s)} = \frac{1}{A_T \times f_s} = \frac{T_s}{A_T} \quad (12)$$

Thus, the open loop transfer function of the proposed rectifier system is

$$\hat{G}_{OL}(s) = \frac{\hat{V}_o(s)}{\hat{V}_{con}(s)} = \frac{b_2 s^2 + b_1 s + b_0 T_s}{a_2 s^2 + a_1 s + a_0 A_T} \quad (13)$$

With the above expression stability of the system can be analysed and thereby controller can be designed for the satisfactory closed loop compensation.

4. CONTROL TECHNIQUES

Two types of control techniques employed here is (Pulse Width Modulation (PWM) Technique and Variable Frequency Control Technique. In PWM Control the widths of pulses can be varied to control the output voltage. In variable frequency control the frequency is varied over wide range to obtain the full output voltage range. Figure 4shows the block diagram of the boost rectifier with control where ABS,DIV,and VFC perform operations of absolute value, analog division and voltage to frequency conversion respectively. For an output power P_o=75W the circuit is simulated in MATLAB software with the following specifications: Supply voltage V_s =110V_{rms}; switching frequency f_s= 40 KHz; Output voltage V_o= 200 V; Load resistance R=530 Ω; Inductance L=500 µH; Input capacitance C_i =8 µF and output capacitance C_o= 2700 µF. The boost rectifier operating in discontinuous conduction mode is modeled and simulated using MATLAB/SIMULINK software.

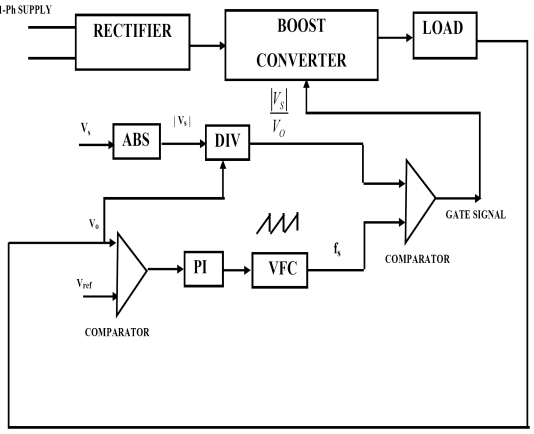

Figure 4: Block Diagram of the Boost Rectifier with the Control

From the open loop result, we conclude that the pulse widths are constant and are shown in Fig.5and to overcome this we have to employ the control technique which eliminates this problem. Here the open loop rectifier model is operating in discontinuous mode of conduction. Input voltage 110 V_{rms} is applied to the rectifier and the rectified output voltage obtained is shown in Fig.6.Here the rectifier feeds the boost converter. The output voltage during closed loop operation is shown in Fig.7. From Fig.8 we infer that the zero crossing of source current & voltage is not same. Also, source current contains harmonics. These harmonics can be reduced by employing the control techniques which are mentioned previously. It is understood that from Fig.9 the zero crossing of the two wave forms are same and harmonics is also reduced approximately around 20% and also the source current follows the sinusoidal nature of the source voltage.The THD value of source current is reduced from 30.47% to 10.45%which as per the IEEE standard there is significant reduction in harmonics.

Journal of Theoretical and Applied Information Technology
31st August 2014. Vol. 66 No.3

ISSN: 1992-8645 www.jatit.org E-ISSN: 1817-3195

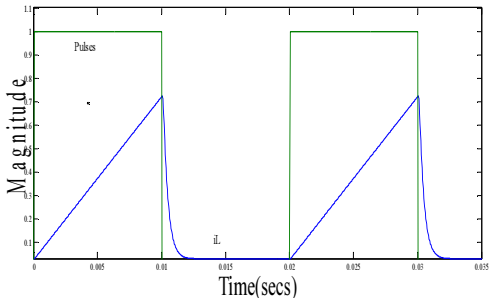

Figure 5: Discontinuous inductor current and gate pulses in open loop

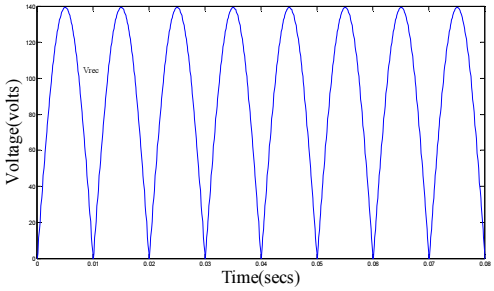

Figure 6: Rectified output voltage

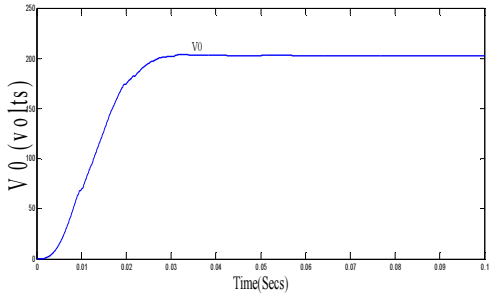

Figure 7: Output voltage in closed loop

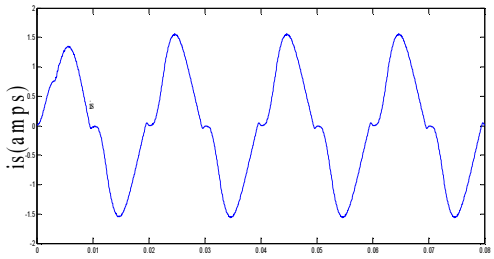

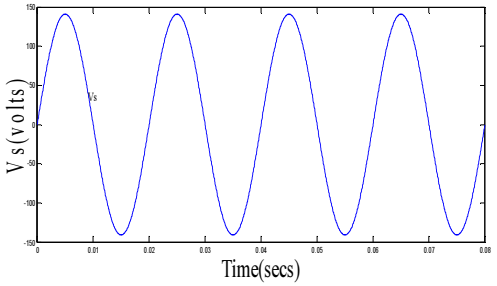

Figure 8: Source current and source voltage in open loop

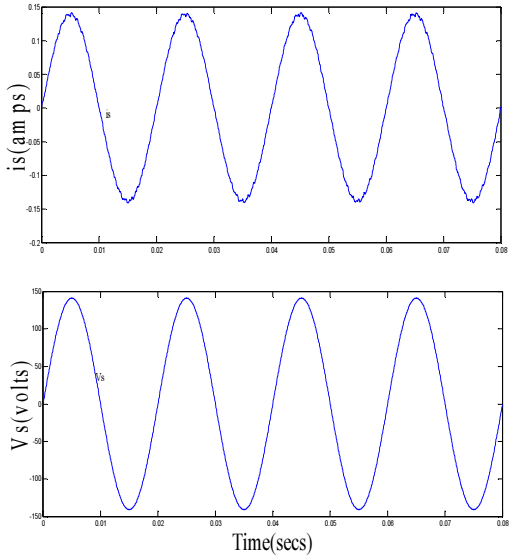

Figure 9: Source current and source voltage in closed loop

5. CONCLUSION

The single phase boost PFC converter has been simulated for the control methods. It is seen that the current harmonics present in the line current has been reduced and zero crossing distortion is also alleviated. The simulation has been done using MATLAB/Simulink. In this work, analysis of discontinuous mode dc-dc boost rectifier has been performed. For this, a state space averaged model is used. It was shown that the pulse widths are getting changed in the closed loop configuration whereas in the open loop system it is not so. The simulated results using MATLAB of boost rectifier under discontinuous conduction mode with control method verifies reduction of the harmonics present in the input current.

ISSN: 1992-8645 www.jatit.org E-ISSN: 1817-3195

REFRENCES:

[1] E. J. P.Mascarenhas, "Hysteresis control of a continuous boost regulator,"in *IEE Colloq. Static Power Convers.*, 1992, pp. 7/1–7/4.

[2] C. Zhou, R. B. Ridley, and F. C. Lee, "Design and analysis of a hysteretic boost power factor correction circuit," in *Proc. IEEE PESC*, 1990,pp. 800–807.

[3] K. H. Liu and Y. L. Lin, "Current waveform distortion in power factor correction circuits employing discontinuous-mode boost converters," in *Proc. IEEE PESC*, 1989, pp. 825–829.

[4] R. Richard, "Reducing distortion in boost rectifiers with automatic control," in *Proc. IEEE APEC*, 1997, pp. 74–80.

[5] D. F. Weng and S. Yuvarajan, "Constant-switching-frequency AC–DC converter using second-harmonic-injected PWM," *IEEE Trans. Power Electron.*, vol. 11, no. 1, pp. 115–121, Jan. 1996.

[6] D. Simonnetti, J. Sebastian, J. A. Cobos, and J. Uceda, "Analysis of the conduction boundary of a boost PFP fed by universal input," in *Proc.IEEE PESC*, 1996, pp. 1204–1208.

[7] Y. K. Lo, S. Y. Ou, andJ. Y.Lin, "Switching frequency control for control for regulated discontinuous conduction mode boost rectifiers," IEEE Trans.Industrial Electron Vol.54 no.2, pp *115-121*Apr 2007.

[8] Y. K. Lo, S. Y. Ou, and T. H. Song, "Varying duty cycle control for discontinuous conduction mode boost rectifiers," in *Proc. IEEE PEDS*, 2001, pp. 149–151.

[9] Kinattingal Sundareswaran and V. T. Sreedevi,"Boost converter controller design using Queen-bee-assisted GA", *IEEE Transactions on industrial electronics*, vol. 56, no. 3, March 2009.

[10] G. Seshagiri Rao, S. Raghu, and N. Rajasekaran, "Design of Feedback Controller for Boost Converter Using Optimization Technique'',International Journal of Power Electronics and Drive System(IJPEDS) Vol. 3, No. 1, pp. 117-128,March 2013.

[11] T.Ajith Bosco Raj and R.Ramesh , "Modelling and Analysis of Parallel Boost Converter for Photovoltaic Applications'' Journal of Theoretical and Applied Information Technology,2014,Vol.62,n0.2pp.309-316.